Model Comparison in Plasma Energy Confinement Scaling revisited

R. Preuss, A. Dinklage

Max-Planck-Institut für Plasmaphysik
EURATOM Association, D-85748 Garching, Germany
preuss@ipp.mpg.de

Abstract. Already in 1998 we presented on a MaxEnt conference a Bayesian model comparison for the confinement scaling of fusion devices [1]. The reason to visit this field again is an over the years enlarged data basis facilitating new physical insights. We compare up to ten physical models on the basis of the old (low-β) data of the 1998 approach and newly acquired high-β data. This work serves as an example where the prior odds cannot be set constant (as would be the normal procedure) but has to be furnished with physics information.

INTRODUCTION

In the work of 1998 [1] we examined confinement data of one of the fusion devices in Garching, the W7-AS stellarator. Due to the machine conditions at that time the data was mainly of collisional low-β character (where β is the ratio of the kinetic pressure of the plasma and the magnetic field pressure exerted by the toroidal magnetic field). The type of the data was successfully identified by a model comparison from a choice of four models distinguishing between collisionless/collisional and low-/high-β plasma. Furthermore, the method was capable of predicting the outcome of single variable scans not contained in the data base. Since then, several experimental campaigns in W7-AS have explored the high-β regime. It is expected that the interpretation of these new data requires a different description and hence a new model is necessary as compared to the low-β regime.

The physical models emerge from dimensional constraints on the exponents of a scaling function over the confinement energy W. These dimensional constraints are related, e.g., to the influence of collisions among the plasma particles, charge neutrality or β. As operation parameters entering the scaling function serve the electron density n, toroidal magnetic field B, absorbed power P and the effective minor radius a

$$W^{theo} \propto n^{\alpha_n} B^{\alpha_B} P^{\alpha_P} a^{\alpha_a} \ . \tag{1}$$

The invariance principle of Connor and Taylor [2] states that if the confinement of plasma is described by the equations of some particular plasma model then a confinement time calculated from that model must reflect any invariance properties of those equations, no matter how complex the calculation. Thus by examining the linear transformation behavior of such basic equations like the Fokker-Planck equation or Maxwell equations one can derive constraints on the above scaling exponents. For instance, tak-

TABLE 1. Connor-Taylor models. The last column shows the respective number of variables in the model (dof: degree of freedom).

CT-model M_j	Abbr.	ξ_1	ξ_2	ξ_3	ξ_4	N_{dof}
Collisionless low-β	L	x	0	0	0	1
Collisional low-β	CL	x	y	0	0	2
Collisionless high-β	H	x	0	z	0	2
Collisional high-β	CH	x	y	z	0	3
Non-neutral collisionless low-β	NL	x	0	0	w	2
Non-neutral collisional low-β	NCL	x	y	0	w	3
Non-neutral collisionless high-β	NH	x	0	z	w	3
Non-neutral collisional high-β	NCH	x	y	z	w	4
Ideal fluid	FI	x	0	1-x/2	0	1
Resistive fluid	FR	x	y	1-x/2+y	0	2

ing the Fokker-Planck equation into account without a term reflecting collisions among the plasma particles and without obedience to Maxwell equations, the simplest Connor-Taylor (CT) model, i.e. collisionless low-β, evolves. By gradually switching on a collision term, Ampere's law (for high-β) and/or Poisson's equation (for non-neutrality) a variety of eight models is obtained. Additionally, we examine two fluid models described by continuity, momentum and energy equation with a choice of ignoring dissipative effects which leads to either ideal or resistive fluid model. The respective constraints on the scaling exponents yield the following scaling law ansatz where the assignment to the specific model is shown in table 1.

$$W^{theo} \propto na^4B^2\left(\frac{P}{na^4B^3}\right)^{\xi_1}\left(\frac{a^3B^4}{n}\right)^{\xi_2}\left(\frac{1}{na^2}\right)^{\xi_3}\left(\frac{B^2}{n}\right)^{\xi_4} \tag{2}$$

$$= cf(\boldsymbol{\xi}) . \tag{3}$$

c is the proportionality constant and $f(\boldsymbol{\xi})$ comprises the terms with the scaling exponents $\boldsymbol{\xi} = (\xi_1,...,\xi_{N_{dof}})$. Note that the number N_{dof} of the latter varies between one and four, e.g. in the simplest case of the collisionless low-β model there is only one scaling exponent $\xi_1 = x$.

One of the achievements of the 1998 approach was to overcome a shortcoming of common scaling laws, i.e. the failure to mimic the saturation of confinement with n or P. This follows from exploiting the invariance principle one step further and to scale not over a single term but over a sum of scaling terms $f(\boldsymbol{\xi}_k)$ with expansion coefficients c_k.

$$W^{theo} = \sum_{k=1}^{E} c_k f(\boldsymbol{\xi}_k) . \tag{4}$$

Since a sum is a linear operation the transformation properties of Eq. (3) are conserved. Which expansion order E is necessary to describe the data best is in the realm of Occam's razor self-consistently contained in Bayesian model comparison.

MODEL COMPARISON

A thorough discussion of the uncertainties of the measured quantities is of major importance for the identification of the most appropriate model. This was already part of the work in 1998 and pursued on last years conference [3]. As we are confident that the qualitative description has come to an end, we would still like to introduce an overall correction factor ω in order to allow for deviations on the quantitative level. For a set of N data this leads to the following likelihood function

$$p(\boldsymbol{W}^{exp}|\omega, \boldsymbol{c}, \boldsymbol{x}, E, M_j, \boldsymbol{\sigma}, I) = \left(\frac{\omega}{2\pi}\right)^{\frac{N}{2}} \frac{1}{\prod_i^N \sigma_i}$$

$$\cdot \exp\left\{-\omega \sum_{i=1}^N \frac{\left[W_i^{exp} - \sum_k^E c_k f_i(\boldsymbol{x}_k)\right]^2}{2\sigma_i^2}\right\} . \tag{5}$$

The uncertainty $\boldsymbol{\sigma}$ of the energy content $\boldsymbol{W}^{exp}$ contains the direct distributions from the diamagnetic measurement as well as indirect contributions from the finite precision in the input variables (n, B, P, a).

We are looking for the probability of a model M_j given the data $\boldsymbol{W}^{exp}$. The odds ratio reads

$$\frac{p(M_j|\boldsymbol{W}^{exp}, \boldsymbol{\sigma}, I)}{p(M_k|\boldsymbol{W}^{exp}, \boldsymbol{\sigma}, I)} = \frac{p(M_j|\boldsymbol{\sigma}, I)}{p(M_k|\boldsymbol{\sigma}, I)} \frac{p(\boldsymbol{W}^{exp}|M_j, \boldsymbol{\sigma}, I)}{p(\boldsymbol{W}^{exp}|M_k, \boldsymbol{\sigma}, I)} . \tag{6}$$

While normally the prior odds (first ratio on the r.h.s.) is set constant for being ignorant to the preference of a model prior to data, doing so we will face this time a situation where we have reason to change this procedure (s. results section). For the second ratio, the so-called Bayes factor, we have to calculate the global likelihood. This is given by a discrete sum over all expansion orders of Eq. (4)

$$p(\boldsymbol{W}^{exp}|M_j, \boldsymbol{\sigma}, I) = \sum_E p(E|M_j, \boldsymbol{\sigma}, I) p(\boldsymbol{W}^{exp}|E, M_j, \boldsymbol{\sigma}, I) , \tag{7}$$

where $p(E|M_j, \boldsymbol{\sigma}, I)$ is set constant because a priori no expansion order is favored. $p(\boldsymbol{W}^{exp}|E, M_j, \boldsymbol{\sigma}, I)$ is obtained by marginalizing over c, ω and the scaling exponents summarized by a vector $\boldsymbol{\xi}$ with $E \times N_{dof}$ elements

$$p(\boldsymbol{W}^{exp}|E, M_j, \boldsymbol{\sigma}, I) = \int p(\boldsymbol{W}^{exp}|\omega, \boldsymbol{c}, \boldsymbol{\xi}, E, M_j, \boldsymbol{\sigma}, I)$$

$$\cdot \quad p(\omega, \boldsymbol{\xi}, \boldsymbol{c}|E, M_j, \boldsymbol{\sigma}, I) \, \mu(\omega, \boldsymbol{\xi}, \boldsymbol{c}) \, d\omega \, d\boldsymbol{c} \, d\boldsymbol{\xi} , \tag{8}$$

featuring the Riemannian metric $\mu(\omega, \boldsymbol{\xi}, \boldsymbol{c}) = \sqrt{\det[\mathbf{g}]}$ and $|\mathbf{g}|$ as the determinant of the Fisher information matrix [4]. The invariant measure for expansion order E and model with N_{dof} variables is

$$\mu(\omega, \boldsymbol{\xi}, \boldsymbol{c}) = \sqrt{\frac{N}{2}} \, \omega^{\frac{E \cdot N_{dof}}{2} - 1} |\mathbf{C}|^{N_{dof}} |\tilde{\boldsymbol{\Delta}}|^{N_{dof} + 1} \Xi(\boldsymbol{\xi}) , \tag{9}$$

with

$$\Xi(\boldsymbol{\xi}) = \left| \left\{ \left[\mathbf{U}^T \mathbf{L}^{(i)} \left(\mathbb{1} - \mathbf{U}\mathbf{U}^T \right) \mathbf{L}^{(i')} \mathbf{U} \right]_{kk'} \right\} \right|^{N_{dof}} . \tag{10}$$

$\mathbf{C}$ is an $E \times E$ matrix with the expansion coefficients c_k of Eq. (4) on its diagonal. $\tilde{\boldsymbol{\Delta}}$ and $\mathbf{U}$ stem from the singular value decomposition of the $N \times E$ matrix $\mathbf{F}$ (with the E vectors $\boldsymbol{f}(\boldsymbol{x}_k)$ as columns). The matrix $\mathbf{L}^{(i)}$ is an $N \times N$ diagonal matrix consisting of the logarithms of the i-th CT-term in parentheses in (2), $\mathbf{L}^{(i)} = \mathbf{diag}\left(\ln S_\nu^{(i)} \right)$. The column (row) element of the complete $(E \cdot N_{dof}) \times (E \cdot N_{dof})$ matrix in the curly brackets in (10) is obtained by running over all possible i (i') for each k (k') of the expansion in (4).

In the determination of the prior function we choose for $\boldsymbol{\xi}$ a flat prior and Jeffreys' prior for ω with lower and upper boundaries motivated by information from physics. For the coefficients $\boldsymbol{c}$ let us have a look at the χ^2-term in the likelihood function (5). Its minimum value is

$$\chi^2_{min} = \tilde{\boldsymbol{W}}^{exp^T} \tilde{\boldsymbol{W}}^{exp} - \boldsymbol{c_{ML}}^T \tilde{\mathbf{F}}^T \tilde{\mathbf{F}} \boldsymbol{c_{ML}} . \tag{11}$$

The tilde denotes that the i-th vector entry is divided by its respective uncertainty σ_i and $\boldsymbol{c_{ML}}$ is the usual maximum likelihood solution. Since Eq. (11) cannot drop below zero we have

$$\tilde{\boldsymbol{W}}^{exp^T} \tilde{\boldsymbol{W}}^{exp} \geq \boldsymbol{c_{ML}}^T \tilde{\mathbf{F}}^T \tilde{\mathbf{F}} \boldsymbol{c_{ML}} . \tag{12}$$

While (12) is valid for $\boldsymbol{c} = \boldsymbol{c_{ML}}$ only, we can extend its form to an estimation for arbitrary coefficients $\boldsymbol{c}$. For those the right hand side of (12) has to allow for the uncertainties in the data. In order to establish a new upper limit we add $\boldsymbol{\Sigma}^T\boldsymbol{\Sigma}$ to the left hand side of (12)

$$\tilde{\boldsymbol{W}}^{exp^T} \tilde{\boldsymbol{W}}^{exp} + \boldsymbol{\Sigma}^T\boldsymbol{\Sigma} \geq \boldsymbol{c}^T \tilde{\mathbf{F}}^T \tilde{\mathbf{F}} \boldsymbol{c} . \tag{13}$$

A conservative approximation of $\boldsymbol{\Sigma}$ is to assume that the deviation of the expansion from the measured data shall not be larger than the data value itself, which means $\boldsymbol{\Sigma} = \tilde{\boldsymbol{W}}^{exp}$ and results in

$$2\tilde{\boldsymbol{W}}^{exp^T} \tilde{\boldsymbol{W}}^{exp} \geq \boldsymbol{c}^T \tilde{\mathbf{F}}^T \tilde{\mathbf{F}} \boldsymbol{c} . \tag{14}$$

We name this Bessel prior because (12) is nothing but the Bessel inequality if $\tilde{\mathbf{F}}$ would be a complete orthonormal basis. This just imposes an upper boundary on the choice of possible coefficients. We write the Bessel prior as a θ-function which allows only those values for $\boldsymbol{c}$ which fulfill (14)

$$p(\boldsymbol{c}|\boldsymbol{\xi}, E, M_j, \boldsymbol{\sigma}, I) \propto \theta \left(1 - \frac{\boldsymbol{c}^T \tilde{\mathbf{F}}^T \tilde{\mathbf{F}} \boldsymbol{c}}{2\tilde{\boldsymbol{W}}^{exp^T} \tilde{\boldsymbol{W}}^{exp}} \right) . \tag{15}$$

After stating the complete prior function, the next task is the evaluation of its normalization constant Z given by

$$Z = \int p(\omega, \boldsymbol{\xi}, \boldsymbol{c}|E, M_j, \boldsymbol{\sigma}, I) \, d\mu(\omega, \boldsymbol{\xi}, \boldsymbol{c}) = \sqrt{\frac{N}{2}} \int d\boldsymbol{\xi} \, \Xi(\boldsymbol{\xi}) \cdot$$

$$
\cdot \quad \int_{-\infty}^{\infty} d\boldsymbol{c}\, |\tilde{\boldsymbol{\Delta}}|^{N_{dof}+1} |\mathbf{C}|^{N_{dof}} \theta\left(\frac{1 - \boldsymbol{c}^T \tilde{\mathbf{F}}^T \tilde{\mathbf{F}} \boldsymbol{c}}{2\tilde{\boldsymbol{W}}^{exp^T} \tilde{\boldsymbol{W}}^{exp}}\right) \int_{\omega_0}^{\omega_1} d\omega\, \omega^{\frac{E \cdot N_{dof}}{2} - 1}
$$

$$
= \quad \sqrt{\frac{N}{2}} \int d\boldsymbol{\xi}\, \Xi(\boldsymbol{\xi}) \cdot Z_{Bessel} \cdot Z_\omega \, , \tag{16}
$$

where the integration over $\boldsymbol{\xi}$ has to be postponed to the final integration of the posterior function. For the contribution from the ω integration we employ the conservative approximation that our estimation of the experimental error is correct in quantitative respect at least by a factor of two. Since the error enters the problem in a quadratic manner this means that the overall correction factor is something between $\omega_0 = 1/2^2$ and $\omega_1 = 2^2$. Inserting these values in the integration limits of (16) results in

$$
Z_\omega = \frac{2^{EN_{dof}+1}}{EN_{dof}}\left(1 - 4^{-EN_{dof}}\right) \, . \tag{17}
$$

The integral in $\boldsymbol{c}$ covers $-\infty$ to ∞ and the upper limit established by the Bessel prior becomes effective. The term $\boldsymbol{c}^T \tilde{\mathbf{F}}^T \tilde{\mathbf{F}} \boldsymbol{c}$ in the θ function constitutes an ellipsoidal sphere in phase space. In order to calculate the volume of this hyper-sphere we perform a transformation for the principle axes and require $|\tilde{\mathbf{F}}^T \tilde{\mathbf{F}}| \approx |\tilde{\boldsymbol{\Delta}}|^2$. With this approximation we get from the integration over $\boldsymbol{c}$

$$
Z_{Bessel} = \frac{\Gamma\left(\frac{E(N_{dof}+1)}{2}\right)}{\Gamma\left(\frac{N_{dof}+1}{2}\right)^E}\left(2\tilde{\boldsymbol{W}}^{exp^T} \tilde{\boldsymbol{W}}^{exp}\right)^{-\frac{E(N_{dof}+1)}{2}} \, . \tag{18}
$$

Knowing the normalization of the prior function we marginalize over $\boldsymbol{c}$ and ω in (8) and obtain eventually

$$
p(\boldsymbol{W}^{exp}|E, M_j, \boldsymbol{\sigma}, I) \quad = \quad \frac{1}{\prod \sigma_i} \pi^{-\frac{N-E}{2}} 2^{\frac{EN_{dof}}{2}} \frac{1}{Z_\omega Z_{Bessel}} \Gamma\left(\frac{N - E(N_{dof}+1)}{2}\right)
$$

$$
\cdot \int d\boldsymbol{\xi} \quad \hat{\Xi}(\boldsymbol{\xi}) \quad \frac{|\mathbf{C}^{\mathbf{ML}}|^{N_{dof}} |\tilde{\boldsymbol{\Delta}}|^{N_{dof}}}{\left(\tilde{\boldsymbol{W}}^{exp^T} \tilde{\boldsymbol{W}}^{exp} - \boldsymbol{c_{ML}}^T \tilde{\mathbf{F}}^T \tilde{\mathbf{F}} \boldsymbol{c_{ML}}\right)^{\frac{N - E(N_{dof}+1)}{2}}} \, , \tag{19}
$$

with $\hat{\Xi}(\boldsymbol{\xi}) = \Xi(\boldsymbol{\xi}) / \int d\boldsymbol{\xi}'\, \Xi(\boldsymbol{\xi}')$. $\mathbf{C}^{\mathbf{ML}}$ is still the $E \times E$ diagonal matrix from (9) but now with the maximum likelihood values $\boldsymbol{c_{ML}}$ as elements.

The final integration over $\boldsymbol{\xi}$ is performed with Markov chain Monte Carlo techniques employing the thermodynamic integration scheme [5].
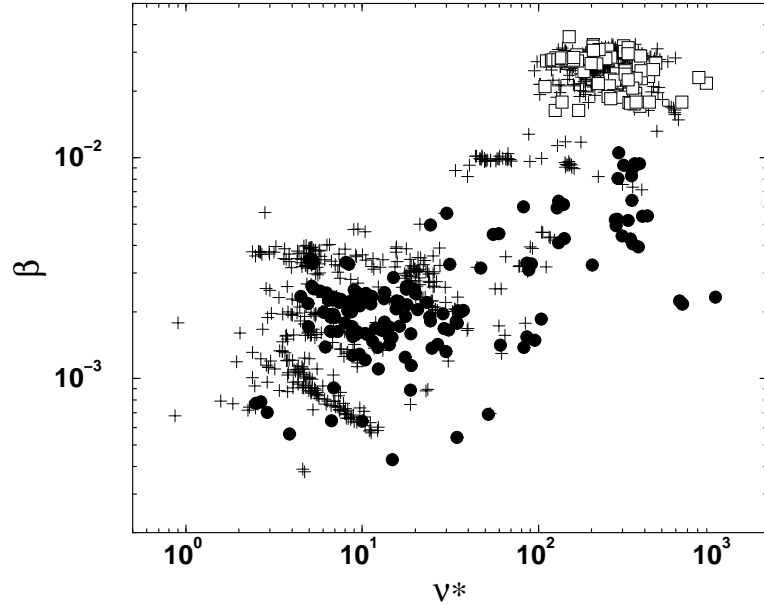
FIGURE 1. W7-AS confinement data as a function of β and collisionality ν^*: low-β subset (circle), high-β subset (squares), additional data in ISCDB (plus signs).

QUALIFYING DATA SUBSETS

Fig. 1 depicts the distribution of a total of 972 entries of W7-AS to the International Stellarator Confinement Data Base (ISCDB) [6] as a function of β and collisionality[1] ν^*. From these data covering different physical regimes subsets with model specific properties have to be selected.

The data set of the previous work (full circles in Fig. 1) was well located in the low-β regime ($\beta \lesssim 1\%$) to serve as a test example for a choice of low- and high-β models. Moreover, for most of these data it was expected that collisions among particles play a role. Additional care has to be taken as the plasma energy W shows a variation of a factor up to two as a function of the rotational transform ι [7]. This necessitates identifying regions in ι with small changes in the absolute value of W (a variation of 10% of the total value was considered as tolerable). For the low-β case, W7-AS shots with ι between 0.33 and 0.35 were chosen resulting in $N = 153$ data.

In order to test the procedure in the high-β range as well, the shot files of W7-AS were subjected to a high-β survey. The search criteria were to consider certain magnetic field and plasma current conditions of shot files in high-β campaigns. Although the influence of ι is expected to be less for the high-β case, a range for ι between 0.45 and 0.49

---

[1] The collisionality ν^* is a dimensionless number to quantify the number of collisions among plasma particles. Its relative size characterizes different regimes where collisions become important for the confinement properties. In the present example of the W7-AS stellarator this is the case for low ($\nu^* \lesssim 20$) and high ($\nu^* \gtrsim 200$) values, but lesser for intermediately valued ν^*.
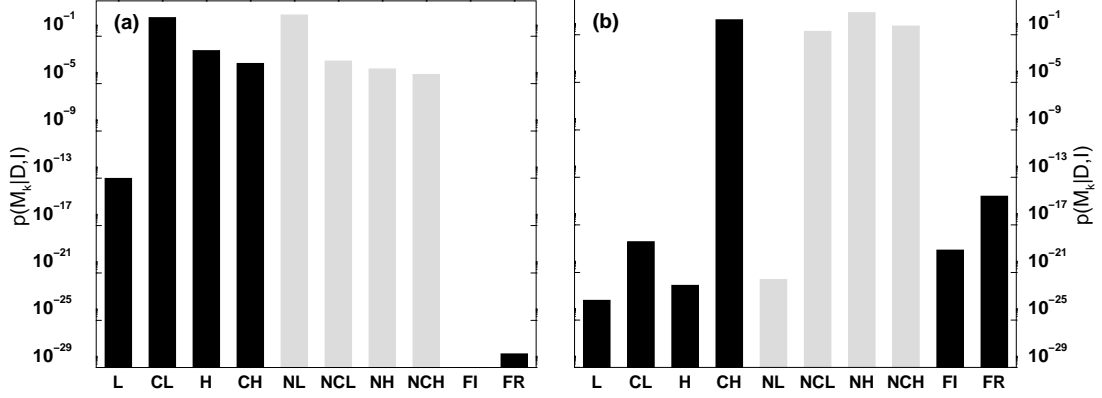
FIGURE 2. Bar chart of the model probabilities for the (a) low-β and (b) high-β data set. The unphysical non-neutral models are shown in gray.

was taken containing N=96 high-β data (open squares in Fig. 1) with still a moderate variation of W according to [7].

RESULTS

The results of the model comparisons are shown in Fig. 2. For the low-β data the outcome of the first four models is a restatement of the work of 1998 with the collisional low-β model as the most probable one. However, with the introduction of non-neutrality, i.e. taking into account the transformation invariances of Poisson's equation with a charge density not equal to zero, surprisingly the non-neutral collisionless low-β model wins. While for length scales below the so-called Debye length the explicit charge distribution of ions and electrons has to be taken into account, above that limit a plasma appears from the outside as being charge neutral. For the machine settings the experiments were performed at it is not expected that phenomena occur which harm the charge neutrality to an extent large enough to show up in global confinement properties. The explanation to this astonishing result can be found by having a closer look at the CT-terms assigned to the specific models. Both models deviate only by exchanging the collisionality-term a^3B^4/n with the non-neutrality-term B^2/n. However, the low-β data hardly vary in a^3B^4 and B^2 making differences between both models blind to model comparison. The magnetic field has only two settings at 2.5T and 1.25T with minor variations around these values, while the minor radius has most of its entries around 12cm and 17.5cm with a few measurements in between. The same happens for the high-β case. Here the (unphysical) non-neutral collisionless high-β model challenges the collisional high-β one. With magnetic fields close to 1.2T and a strong accumulation of the minor radius around 11.7cm again the data base does not offer the possibility to distinguish between both models. These findings are supported by the linear correlation coefficients being significant for the responsible two terms (see table 2).

TABLE 2. Linear correlation coefficient of the CT-terms in Eq. (3) for low- and high-β data.

Data	$\left(\frac{a^3 B^4}{n}, \frac{1}{na^2}\right)$	$\left(\frac{a^3 B^4}{n}, \frac{B^2}{n}\right)$	$\left(\frac{1}{na^2}, \frac{B^2}{n}\right)$
low-β	-0.11	0.84	0.38
high-β	-0.57	0.88	0.15

CONCLUSION

Taking advantage of the invariance principle in order to generate testable models, one has to be cautious that the data base possesses enough variability in the model determining quantities. However, in Bayesian data analysis we have the tool to correct an implausible outcome, i.e. the prior odds ratio. Since the assumption of a plasma without charge neutrality is unphysical the prior odds ratio can be adjusted accordingly. But what is unphysical in numbers? Giving a chance of 1 in 5 does already suffice to obtain the correct result in the above case. Probabilities like $p(M_k|\text{unphysical}) = 10^{-3}$ or lower may be more justified from an expert view.

Apart from this caveat Bayesian model comparison does again detect the correct model (collisional high-β) for a newly acquired high-β data set in the collisional regime. Since the models simply emerge out of an invariance principle regarding the linear transformation behavior of basic physics equation, the procedure seems to be a promising tool whenever the complexity of a problem denies a detailed description.

ACKNOWLEDGMENT

REFERENCES

1. Preuss, R., Dose, V., and von der Linden, W., "Model comparison in plasma energy confinement scaling," in *Maximum Entropy and Bayesian Methods*, edited by V. Dose et al., Kluwer Academic, Dordrecht, 1999.
2. Connor, J. W., and Taylor, J. B., *Nucl. Fusion*, **17**, 1047 (1977).
3. Preuss, R., and Dose, V., "Errors in all variables," in *Bayesian Inference and Maximum Entropy Methods in Science and Engineering*, edited by K. Knuth et al., AIP, Melville, N.Y., 2005, vol. 803 of *AIP Conference proceedings*, p. 448.
4. Rodriguez, C., "From Euclid to entropy," in *Maximum Entropy and Bayesian Methods*, edited by J. W. T. Grandy, Kluwer Academic, Dordrecht, 1991.
5. von der Linden, W., Preuss, R., and Dose, V., "The prior predictive value," in *Maximum Entropy and Bayesian Methods*, edited by V. Dose et al., Kluwer Academic, Dordrecht, 1999.
6. URL of ISCDB: http://www.ipp.mpg.de/ISS and http://iscdb.nifs.ac.jp/.
7. Brakel, R., et al., *Nucl. Fusion*, **42**, 903 (2002).